Macromolecules

Article

pubs.acs.org/Macromolecules

Mobility of Nanoparticles in Semidilute Polyelectrolyte Solutions

Firoozeh Babaye Khorasani, Ryan Poling-Skutvik, Ramanan Krishnamoorti,* and Jacinta C. Conrad*

Department of Chemical and Biomolecular Engineering, University of Houston, Houston, Texas 77204-4004, United States

Supporting Information

ABSTRACT: We measure the mobility of nanoparticles at low concentrations in non-Newtonian semidilute aqueous solutions of high-molecular-weight polyelectrolyte polymers. Using optical microscopy and particle tracking algorithms, we image and track hydrophilic polystyrene nanoparticles of diameter 400 nm moving in aqueous solutions of partially hydrolyzed polyacrylamide of molecular weight 8 000 000 Da and concentration of 0.042—4.2 g/L. The effective diffusivity of the nanoparticles in the semidilute polymer solutions, extracted from the long-time limit of the mean-squared displacement using the Stokes−Einstein relation, is greater than that calculated from the zero-shear-rate viscosity measured using bulk rheology. For concentrations $c > 0.42$ g/L, the mean-square displacements (MSD) of particles measured as a function of lag time revealed that the particle dynamics are subdiffusive at short time scales and are Fickian on long time scales. The time scale for the crossover from subdiffusive to Fickian dynamics increases with increasing polymer concentration; moreover, it is longer than the relaxation time scale for polymer blobs and shorter than that for the chain. Our results suggest that the nanoparticle dynamics are coupled to those of the polymers on a length scale intermediate between the blob size and the end-to-end distance of the polymer.

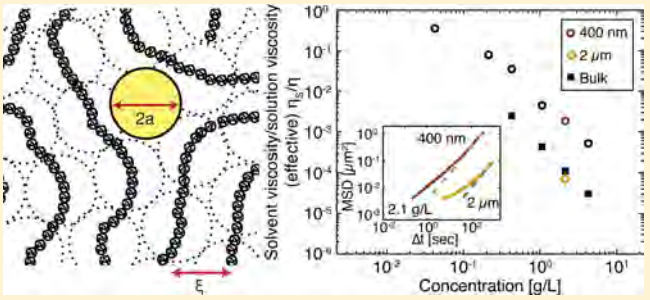

INTRODUCTION

Understanding the mobility of nanoparticles in polymer solutions is required to optimize their transport properties for wide-ranging applications in enhanced oil recovery and polymer nanocomposites. For example, nanoparticles employed to increase oil recovery, through change in the wettability of rock surfaces or through profile control or conformance control, must be transported as components of a polymer-laden fluid to particular regions of the reservoir.[1−3] Similarly, attaining the optimal thermal, mechanical, electrical, and/or optical properties of polymer nanocomposites[4,5] requires excellent control over the distribution of nanoparticles during processing in polymer solutions or melts.[6,7] Likewise, conferring self-healing properties[8−12] to polymer nanocomposites requires mobile nanoparticles within a polymer matrix. In these examples, polymers within a solution or melt may hinder and confine the mobile nanoparticles. Despite these important practical applications, the fundamental mechanisms that influence nanoparticle mobility in polymer solutions remain poorly understood.

Particle mobility is best understood in the limit for larger submicron particles moving in a continuous medium. In a purely viscous solvent, submicron particles undergo Brownian diffusion. Their one-dimensional ensemble-averaged mean-square displacement (MSD) $\langle \Delta x^2(\Delta t)\rangle = \langle (x(t + \Delta t) - x(t))^2\rangle$ scales linearly with the lag time, i.e., $\langle \Delta x^2(\Delta t)\rangle = 2D\Delta t$. The diffusion coefficient D is related to the viscosity η of the background solvent through the Stokes−Einstein relation, $D = k_B T/3\pi\eta d$, where d is the diameter of the particle. Upon addition of polymer, the medium becomes viscoelastic rather than purely viscous and the motion of the particle probes both the elastic response as well as the viscous dissipation of the medium. In this scenario, the Stokes−Einstein relation for the diffusion coefficient is generalized to include a frequency-dependent viscosity, i.e., $D(s) = k_B T/3\pi d s\tilde{\eta}(s)$.[13,14] The generalized Stokes−Einstein relation (GSER) thus allows the complex viscosity to be extracted from the mean-squared displacements of tracer particles. Excellent agreement between macro- and microrheology, using micron-sized particles, has been reported for a wide variety of cross-linked and entangled polymer solutions.[15−25]

The validity of the GSER depends in part on a key underlying assumption, namely that the medium can be treated as a homogeneous continuum. When the size of the particle is much larger than typical length scales in the polymer solution (for example, the polymer radius of gyration in dilute solutions, the end-to-end distance in polyelectrolyte solutions, and the correlation length in semidilute solutions), this assumption is satisfied and particle diffusion is related to the macroscopic rheology through the GSER. When the size of nanoparticles is comparable to or smaller than length scales in the polymer solution, however, the medium cannot be treated a homogeneous continuum. Indeed, the dynamics of nanoparticles in polymer solutions in this regime exhibit nontrivial and noncontinuum dependencies on the characteristics of the polymer solution.[26−33] As one example, the diffusion

Received: June 16, 2014
Revised: July 10, 2014
Published: July 22, 2014

   dx.doi.org/10.1021/ma501248u | Macromolecules 2014, 47, 5328−5333

coefficients of nanometer-scale particles in concentrated and entangled solutions are significantly *higher* than expected based on the bulk solution viscosity.[28,31,33] Both theoretical models and simulations[34−37] developed to explain these surprising results suggest that in concentrated solutions polymer entanglements play a critical role in controlling the nanoparticle dynamics. Polymer fluctuations on length scales ranging from individual chains[35] to the blob size[36] also impact nanoparticle dynamics. Even when the polymers are not entangled, however, they can act as mobile and compressible obstacles[38] through which the particles must diffuse.[39] This effect, termed macromolecular crowding,[40] can also lead to anomalous diffusion[41−47] through caging. Despite extensive work, how these competing mechanisms affect the motion of nanoparticles in polymer solutions remains poorly understood.

In this paper, we investigate the mobility of nanoparticles in aqueous semidilute solutions of high molecular weight hydrolyzed polyacrylamide of concentration 0.042—4.2 g/L; the overlap concentration c^*, based on the intrinsic viscosity, is 0.097 g/L. The diameter of the nanoparticles (∼400 nm) is smaller than the end-to-end distance of the polyelectrolyte polymers in dilute solution (∼775 nm), significantly larger than the Kuhn segment length (∼1 nm), and for the semidilute solutions larger than or comparable to the correlation length (∼95−420 nm). We find that the mean-squared displacement (MSD) is subdiffusive at short time scales for solutions of concentration $c > 0.42$ g/L and exhibits Fickian diffusion on longer time scales. The diffusion coefficient extracted from the long-time slope of the MSD, however, is larger than that calculated from the macroscopic zero-shear-rate viscosity of the polymer solution measured using bulk rheology. This result suggests that the effective viscosity experienced by the nanoparticles is less than that measured in bulk rheology, as also previously found for nanometer-scale particles in polymer solutions.[28,29,31] Moreover, the experimental time scales for the crossover to Fickian dynamics are much longer than those predicted using models that couple the dynamics of the nanoparticles to those of polymer blobs.[35] Our results are consistent with caging of the nanoparticles by polymer segments: the crossover to diffusive dynamics appears upon relaxation of a polymer region of size intermediate between the blob size and the end-to-end distance, and the long-time diffusivity reflects the shear thinning of the solution at the local deformation rate imparted by the nanoparticles.

MATERIALS AND METHODS

Preparation of Nanoparticle−Polymer Solutions. Fluoro-Max dyed red aqueous fluorescent polystyrene nanoparticles of diameter d = 400 nm and microparticles of diameter $d = 2$ μm were purchased at a concentration of 1 wt % from Thermo Fisher Scientific. These nanoparticles were stabilized in water by addition of trace amounts of surfactant with a carboxylate functionality. The density of the nanoparticles was 1.05 g/cm^3 at 25 °C. The peak excitation and peak emission wavelengths for the fluorescence were 542 and 612 nm, respectively. Hydrolyzed polyacrylamide (HPAM) polymers of weight-averaged molecular weight (M_w) of 8 000 000 Da (FLOPAAM 3330) were obtained from SNF and used as received. The degree of hydrolysis was 25—30% as reported by the manufacturer.

We prepared aqueous solutions of HPAM in double-deionized water with varying concentrations of polymer; the overlap concentration $c^* = 0.097 \pm 0.001$ g/L was estimated from the intrinsic viscosity $[\eta]$ (Supporting Information, Figure S1). For imaging, we prepared solutions at polymer concentrations ranging from 0.042−4.2 g/L, corresponding to 0.67—67c^*. The end-to-end distance in dilute solution $R_0 \approx 775$ nm was calculated using the Fox−Flory equation,[48] $[\eta] = \Phi R^3/M_w$, where Φ is the Flory constant, and the correlation length $\xi/R_0 \sim (c/c^*)^{-1/2}$ was estimated using a scaling relationship for polyelectrolytes.[49] Sample vials were cleaned with three organic solvents (toluene, tetrahydrofuran, and acetone), rinsed with deionized water, and subsequently dried in a convection oven. Appropriate quantities of HPAM and deionized water were added to a cleaned vial to create a solution of known polymer concentration. The solution was then thoroughly mixed by tumbling on a roll mill for between 2 days and 1 week, depending on polymer concentration, until a uniformly homogeneous solution was obtained. Finally, nanoparticles were added to each homogenized solution at a concentration of 0.002 wt % for imaging experiments.

Imaging Protocol. Each sample was confined in a thin glass chamber of thickness ∼0.2 mm to prevent macroscopic motion (Supporting Information). The chamber was filled with 100 μL of sample using a pipet and sealed using UV-curable epoxy. Samples were imaged using a Leica DM4000 inverted microscope equipped with a 100× lens with numerical aperture (NA) of 1.40. Two cameras with distinct ranges of video-capture frame rates were used to image the nanoparticles as they diffused in aqueous HPAM solutions. Movies were acquired at 32, 63, or 120 frames per second (fps) using a AOS Technologies AG camera (S-PRI) with a pixel size of 0.195 ± 0.002 μm and 0.67, 1, 1.67, or 2.5 fps using an Olympus camera (DP21) with a pixel size of 0.1266 ± 0.0012 μm. We acquired multiple movies of each sample at different frame rates and thereby accessed the dynamics of the nanoparticles across a wide range of time scales (0.008—450 s).

Particle Tracking. We used particle-tracking algorithms[50] to locate and track the nanoparticles in a time series of fluorescence micrographs. Images from a time series were first denoised using a bandpass filter to remove the background intensity. The centroids of all particles were then located with resolution of ε = 40 nm (by refining the locations of the local maxima of intensity) and subsequently linked into trajectories. From the trajectories of the nanoparticles, we calculated the one-dimensional ensemble-averaged mean-squared displacement (MSD) of the particles $\langle \Delta x^2(\Delta t) \rangle$. Although we measured the dynamics across a wide range of time scales, we reported here only those mean-squared displacements greater than $2\varepsilon^2$ that corresponded to displacements that could be resolved using the tracking technique.

Bulk Rheological Measurements. To measure the rheological properties of the semidilute polymer solutions, we used a TA DHR rheometer equipped with a Couette geometry (cup diameter of 30.36 mm, bob diameter of 27.97 mm, bob length of 41.89 mm, and gap height of 4 mm). Samples were gently loaded into the instrument prior to measurements, and we ensured that no bubbles were present inside the sample after loading. We measured the frequency-dependent linear elastic ($G'(\omega)$) and viscous ($G''(\omega)$) moduli over the frequency range ω = 100−0.01 rad/s (Supporting Information). From the frequency-dependent moduli, we calculated the complex viscosity as $\eta^*(\omega) = [G'^2(\omega) + G''^2(\omega)]^{1/2}/\omega$ and reported the complex viscosity as a function of the frequency.

Polymer solutions of concentration $c \leq 0.42$ g/L did not generate sufficient torque, and we were unable to characterize the full frequency-dependent viscosity for these solutions. Instead, we used two capillary viscometers (sizes 0B and 0C, Cannon 9721-R56 and 9721-R53) to measure the solution viscosity for polymer solutions with concentration $c \leq 0.042$ g/L. Prior to each experiment, the viscometers were rinsed with acetone and deionized water, dried in an oven at 130 °C for 15 min, and cooled by passing nitrogen through the viscometer. The effective shear rates were estimated as $\dot{\gamma} = 8V/D$, where V is the average velocity of the solution moving through the viscometer and D is its diameter, as 297 s^{-1} (0B) and 233 s^{-1} (0C).

Dynamic Light Scattering (DLS). To determine whether the polymers irreversibly adhered to the particles, the hydrodynamic size of the particles as a function of polymer concentration was determined using dynamic light scattering as described in the Supporting Information.

dx.doi.org/10.1021/ma501248u | Macromolecules 2014, 47, 5328−5333

RESULTS AND DISCUSSION

The mobility of the nanoparticles in the polymer solutions, as measured by particle tracking methods, qualitatively and quantitatively changed with increasing polymer concentration as shown in Figure 1. At low concentrations of polymer (0.042 g/L) the dynamics of the nanoparticles were nearly diffusive, as indicated by the linear fits to the mean-squared displacement (MSD) $\langle \Delta x^2(\Delta t) \rangle = 2D\Delta t$ over all time scales. When the polymer concentration was increased above 0.42 g/L, the slope of the MSD as a function of lag time at short times (on a log−log scale) was less than one, indicating the emergence of subdiffusive dynamics on short time scales. Subdiffusive exponents for nanoparticle mobility in neutral polymer solutions are often attributed to entanglements,[31] but entanglement effects in salt-free solutions of high-molecular-weight polyelectrolytes typically do not appear until concentrations that are much larger than c^* (estimated as >1000c^* for a molecular weight of 8 000 000[51]). The slope of the short-time MSD as a function of lag time decreased as the concentration of polymer was increased from ∼0.8 at 0.42 g/L to ∼0.4 at 4.2 g/L. On long time scales the dynamics of the nanoparticles were Fickian diffusive, as indicated by the linear dependence of the MSD on lag time for all samples (0.042—4.2 g/L). The time at which the dynamics exhibited the crossover to Fickian diffusive behavior increased from ∼5 s at 0.42 g/L to ∼30 s at 4.2 g/L. The distributions of particle displacements, however, remained Gaussian on all time scales (Supporting Information, Figures S2—S7). We concluded that on long time scales the nanoparticles diffused in an effective medium and extracted an effective long-time diffusion coefficient D_{eff} for each polymer concentration from the long-time slope of the MSD.

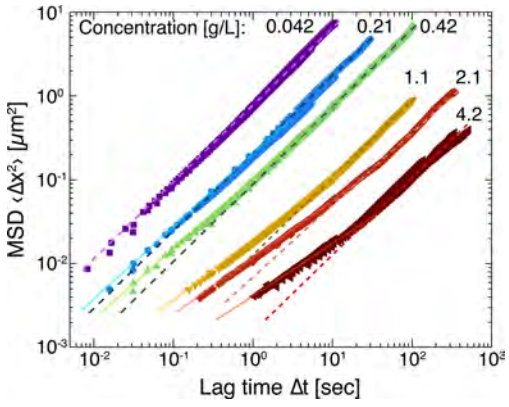

Figure 1. Mean-squared displacement (MSD) $\langle \Delta x^2(\Delta t) \rangle$ as a function of lag time Δt for 400 nm diameter nanoparticles in aqueous solutions of solutions of hydrolyzed polyacrylamide of varying concentration c (in units of g/L). Dashed lines indicate linear fits (power law exponent of one) at long time scales; dotted lines indicate power-law fits with varying exponent at short time scales.

In homogeneous solutions, the diffusion coefficient of particles of diameter d in a homogeneous solution is related to the solution viscosity using the Stokes−Einstein equation, $D = k_B T/3\pi\eta d$, where T is the temperature and η is the viscosity of the solution. We thus compared the effective diffusivity D_{eff}, obtained from the long-time particle tracking data, with that calculated from Stokes−Einstein (D_{SE}), obtained from the measured bulk zero-shear rate viscosity and the known particle diameter. For polymer concentrations greater than 0.42 g/L, we measured the bulk solution viscoelasticity using rheology. The bulk viscosity of the semidilute polymer solutions was strongly shear-thinning, as shown in Figure 2. At low shear rates the viscosity was nearly independent of shear-rate (i.e., Newtonian). We thus extracted the low-shear-rate viscosity that characterized the bulk viscosity in a quiescent solution and thereby calculated D_{SE}. Polymer solutions with concentrations below 0.42 g/L did not generate sufficient torque in the rheometer to allow measurements of the zero-shear-rate viscosity. Instead, we employed capillary viscometry to measure the solution viscosity at a finite shear rate and similarly calculated the effective diffusivity D_{SE} at c = 0.042 g/L.

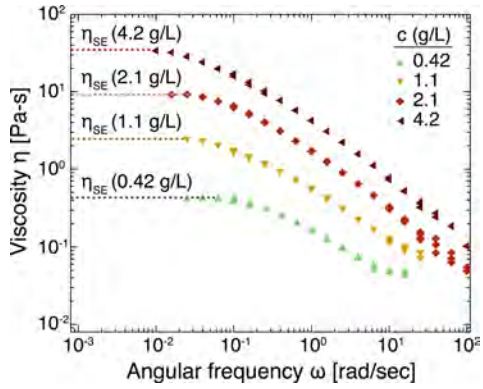

Figure 2. Viscosity η as a function of angular frequency ω for solutions of hydrolyzed polyacrylamide with varying concentration c (in units of g/L), as measured in a double-Couette geometry. The dashed lines indicate the values of the low-shear viscosity η_{SE} extrapolated from the measured viscosity for each concentration.

We observed significant discrepancies between the microscopic D_{eff} and macroscopic D_{SE} for solutions of concentration $c \geq 0.42$ g/L, as shown in Figure 3. For polymer concentrations greater than 0.42 g/L we found that $D_{eff} > D_{SE}$, as was observed for much smaller nanoparticles in polymer solutions and

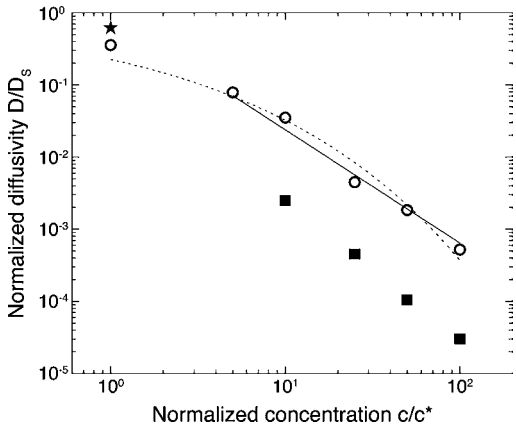

Figure 3. Nanoparticle diffusivity D_{eff}/D_s extracted from the long-time mean-squared displacements as a function of the normalized polymer concentration c/c^* (open symbols). Solid symbols indicate the diffusivity calculated from experimental measurements of the bulk viscosity: squares use the zero-shear viscosity measured for solutions with $c/c^* \geq 6.7$ (corresponding to $c \geq 0.42$ g/L), and the star (c/c^* = 0.67, corresponding to c = 0.042 g/L) uses the viscosity measured at a shear rate of 233 s^{-1} using a capillary viscometer. The dashed and solid lines show fits to models by ref 52 (for all data) and ref 35 (for $c/c^* >$ 1 only), respectively.

dx.doi.org/10.1021/ma501248u | Macromolecules 2014, 47, 5328−5333

melts.[28,33] The ratio $D_{eff}/D_{SE} \sim 10$ was approximately constant over the concentrations probed, similar to that obtained with smaller nanoparticles at comparable $d/R \sim 0.6$ in solutions of neutral polymers.[33] At lower polymer concentrations the discrepancy between D_{eff} and D_{SE} largely vanished. For a polymer concentration of 0.042 g/L we found that D_{SE} was slightly larger than D_{eff}, which we attributed to shear thinning of the polymer solution at the shear rate (233 s^{-1}) at which the viscosity was measured.

The discrepancy between D_{eff} and D_{SE} observed here for the 400 nm diameter nanoparticles, like that observed earlier for smaller nanoparticles,[28,31,33] suggests that the dynamics of nanoparticles of size comparable to the polymer coils do not probe the bulk rheological properties of polymer solutions. Because particles whose size is much larger than characteristic length scales are known to probe the bulk rheology of polymer solutions,[15−25] we measured the mean-squared displacement (MSD) using surfactant-stabilized polystyrene microparticles of diameter 2 μm in a HPAM solution with a polymer concentration of 2.1 g/L. For these particles the ratio of the particle size to the end-to-end distance of the polymers was $d/R \sim 2.5$. For the larger particles the long time MSD dependence was again consistent with diffusive dynamics, as shown in Figure 4. Furthermore, the diffusivity extracted from the long-time slope of the microparticles was much closer to the low-shear-rate viscosity measured using bulk rheology; we attributed the factor of 2 difference in diffusivities (and hence in effective viscosities) to the relatively small $d/R \sim 2.5$ of the microparticles. This experiment indicated that bulk solution viscosity would be recovered as the size of the particles was increased.

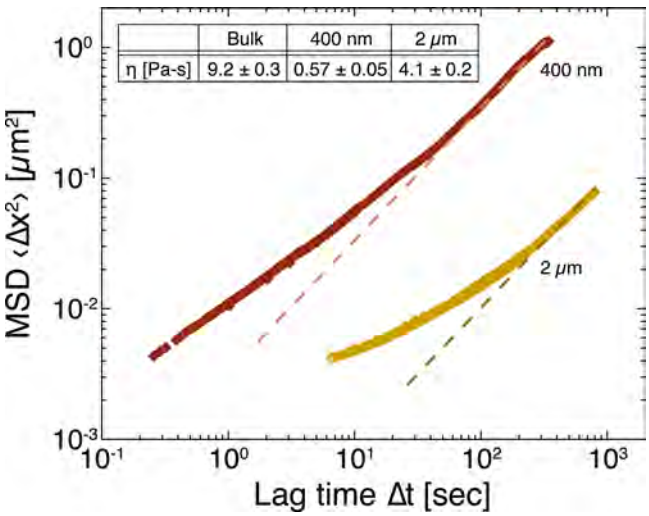

Figure 4. Mean-squared displacement (MSD) as a function of time for particles of diameter 400 nm and 2 μm diffusing in a polymer solution with concentration 2.1 g/L. Inset table: viscosity η extracted from the low-shear-rate bulk rheology and from the long-time limit of the MSD for 400 nm and 2 μm particles.

From the microscopy studies, we summarize two key results for the diffusion of nanoparticles in high-molecular-weight polyelectrolyte solutions. First, for concentrations $c \geq 0.42$ g/L the nanoparticles exhibited subdiffusive dynamics on short time scales. Second, the dynamics of nanoparticles for all solutions were diffusive on long time scales, but the diffusivity extracted from the long-time slope of the MSD was over an order of magnitude larger than that calculated from the zero-shear-rate viscosity of the polymer solutions. We note that the concentration dependence of D_{eff} alone does not provide insight into the mechanisms driving the dynamics: over the range of polymer concentrations probed in this study, both a stretched-exponential model, $D_{eff} \propto \exp(-c^{\nu})$ [ref 52] and a scaling model, $D_{eff} \propto (c/c^*)^{-1.52}$ [ref 35] could describe the concentration dependence of D_{eff}, as shown by the fits in Figure 3.

We first considered several mechanisms for the origin of the subdiffusive dynamics at short times. The first potential mechanism is solution elasticity: micron-sized particles diffusing in entangled or cross-linked polymer solutions exhibit subdiffusive dynamics on short time scales that are coupled to the elasticity of the solution,[16,19] as described quantitatively using the generalized Stokes−Einstein equation.[13] One-point microrheology measurements for the linear elastic and viscous moduli, however, also deviated from the bulk values (Supporting Information, Figure S8). Separately, we note that the polymer concentrations examined here are significantly smaller than those for which the effects of entanglements are observed for polyelectrolyte solutions. We thus contend that the subdiffusive dynamics of the nanoparticles in semidilute polyelectrolyte solutions do not reflect the bulk rheological properties of the solution.

We next considered the possibility that the polymers irreversibly adhered to the nanoparticles, as earlier experiments found that polymer sticking could lead to subdiffusive exponents of ∼0.5 that reflected the Rouse-like dynamics of the polymers.[53,54] To test this idea, we formulated dilute solutions of polymer at concentrations ranging from 0.00084 to 0.027 g/L containing nanoparticles of 400 nm and measured the hydrodynamic radius of the nanoparticles using dynamic light scattering. Within experimental error, the hydrodynamic radius of the particles was constant across the range of polymer concentrations probed (Supporting Information, Figure S9), indicating that the polymers did not strongly interact with the nanoparticles.

Finally, we considered the possibility that the subdiffusive dynamics reflected coupling between particle and polymer dynamics. We tested this idea using the scaling model of Rubinstein and collaborators,[35] which predicts a crossover from subdiffusive to diffusive behavior for particles whose size falls between the correlation length (which we estimate for polyelectrolytes[49] as $\xi/R_0 \sim (c/c^*)^{-1/2}$) and the tube diameter; because our solutions are not entangled, this intermediate regime is the relevant one for our experiments. The time scale for the crossover from subdiffusive to diffusive dynamics obtained from this model, $\tau_d \sim (\eta_s \xi^3/k_B T)(2a/\xi)^4 \sim \eta_s (2a)^4/(k_B T \xi)$, is much shorter than the crossover time scale that we observed in experiments for all polymer concentrations (e.g., for c = 2.1 g/L ($c/c^* \sim 33$), $\tau_d \sim 0.041$ s from the Rubinstein model and the experimental crossover occurs at ∼19 s; estimated time scales for the crossover and for the blob size relaxation are given in Table S1 of the Supporting Information). This comparison suggests that polymer dynamics at the blob and particle scales do not control the particle dynamics.

Instead, we suggest a physical picture for subdiffusive motility in the semidilute regime that is motivated by comparisons to caged or crowded systems. In those systems, subdiffusive particle dynamics can indicate the presence of obstacles that locally cage the particle on short time scales; the transition from

dx.doi.org/10.1021/ma501248u | Macromolecules 2014, 47, 5328−5333

subdiffusive to diffusive motility occurs when this local cage relaxes and the particle escapes. In our semidilute solutions, the nanoparticles are caged by the large polymers. We suggest that the transition to diffusive mobility occurs when the cage formed by the polymers relaxes. This relaxation must occur over multiple blobs because the transition to diffusive motility occurs on longer time scales than τ_d. Similarly, this relaxation must occur on length scales smaller than the end-to-end distance because the transition occurs on shorter time scales than the characteristic time scale for chain diffusion (e.g., for c = 2.1 g/L ($c/c^* \sim 33$), the Rouse time scale is ∼31 s as estimated from Figure 2). These comparisons suggest that the length scale over which the local cage must relax is intermediate between the blob size and the end-to-end distance of the polymer. This length scale may be set by transient clustering[55] between polymer segments, which is thought to generate a slow relaxation in polymer solutions in less-good solvents whose concentration is intermediate between the overlap and entanglement concentrations.

This picture is also consistent with the faster-than-expected mobility of the nanoparticles in the polymer solutions. On long time scales the nanoparticles exhibit free diffusion, but in an effective medium of lower viscosity than the zero-shear-rate bulk viscosity. As before, we note that the faster-than-expected dynamics cannot reflect the viscoelasticity of the polymer solution or nanoparticle−polymer adhesion—indeed, these mechanisms would lead to *slower* mobility. Instead, the lower effective viscosity also reflects the coupling between nanoparticle and polymer dynamics[35] through local relaxation. The local rate at which the nanoparticles deform the polymer matrix is nonzero because the polymer solutions are shear-thinning; the nanoparticles thus experience a viscosity that is lower than that at zero-shear rate.

CONCLUSIONS

We measured the mobility of nanoparticles of diameter 400 nm in solutions of high-molecular-weight hydrolyzed polyacrylamide of end-to-end distance 775 nm. For solutions in which the polymer concentration is greater than the overlap concentration, the dynamics changes from subdiffusive at short time scales to diffusive on long time scales. The time scale at the crossover between these dynamics increases with polymer concentration. The effective diffusivity extracted from the long-time dynamics, however, is always greater than that calculated from the zero-shear-rate bulk viscosity. The lower-than-expected effective viscosities experienced by the nanoparticles (for c > 0.42 g/L) suggest that their dynamics are coupled to polymer fluctuations, as observed and predicted for smaller nanoparticles (∼nm) that sample dynamics on the scale of polymer chain segments. Because the transition from subdiffusive to diffusive mobility occurs on time scales intermediate between the relaxation time scales for polymer blobs and for self-diffusion, we suggest that the length scale controlling the coupling of nanoparticle and polymer dynamics is intermediate between the blob size and the end-to-end distance. On short time scales the nanoparticles are caged by the polymers; on longer time scales this local cage relaxes to allow the nanoparticle to freely diffuse in an effective medium whose viscosity reflects the shear-thinning nature of the polymer solution.

This physical picture suggests an origin for both of the distinctive features of nanoparticle mobility in polyelectrolyte solutions observed here. An open question, however, is the physics that sets the size of the relaxing region that controls the crossover from subdiffusive to diffusive mobility. Similar measurements over a wide range of particle-to-polymer size ratios and particle−polymer interactions are needed to identify this critical length scale and are underway. We note that the static and dynamic behaviors of polyelectrolytes are somewhat more complex than those of polymers due to the presence of charges; in particular, both solvent quality and counterion concentration may significantly affect the polymer dynamics and hence those of the nanoparticles. Nonetheless, we expect these results to have interesting implications for nanoparticle diffusion in a wide range of polymer and polyelectrolyte solutions, including nanoparticle-based strategies to change the interfacial interactions in highly confined porous media to enhance oil recovery and processing strategies to fabricate advanced polymer nanocomposites.

ASSOCIATED CONTENT

Supporting Information

Experimental details; Figures S1−S9 and Table S1. This material is available free of charge via the Internet at http://pubs.acs.org.

AUTHOR INFORMATION

Corresponding Authors

*E-mail: (R.K.) ramanan@uh.edu.
*E-mail (J.C.C.) jcconrad@uh.edu.

Notes

The authors declare no competing financial interest.

ACKNOWLEDGMENTS

R.K. acknowledges the partial support of the Gulf of Mexico Research Initiative (Consortium for Ocean Leadership Grant SA 12-05/GoMRI-002). J.C.C. acknowledges the support of the American Chemical Society Petroleum Research Fund (52537-DNI7) and the National Science Foundation (DMR-1151133).

REFERENCES

(1) Sahimi, M. *Rev. Mod. Phys.* **1993**, *65* (4), 1393−1534.
(2) Ponnapati, R.; Karazincir, O.; Dao, E.; Ng, R.; Mohanty, K. K.; Krishnamoorti, R. *Ind. Eng. Chem. Res.* **2011**, *50* (23), 13030−13036.
(3) Metin, C. O.; Bonnecaze, R. T.; Nguyen, Q. P. *SPE Res. Eval. & Eng.* **2013**, *16* (03), 327−332.
(4) Njuguna, J.; Pielichowski, K.; Alcock, J. R. *Adv. Eng. Mater.* **2007**, *9* (10), 835−847.
(5) Kumar, S. K.; Krishnamoorti, R. *Annu. Rev. Chem. Biomol. Eng.* **2010**, *1* (1), 37−58.
(6) Gam, S.; Meth, J. S.; Zane, S. G.; Chi, C.; Wood, B. A.; Winey, K. I.; Clarke, N.; Composto, R. J. *Soft Matter* **2012**, *8* (24), 2512−2520.
(7) Kim, D.; Srivastava, S.; Narayanan, S.; Archer, L. A. *Soft Matter* **2012**, *8* (42), 10813−10818.
(8) Toohey, K. S.; Sottos, N. R.; Lewis, J. A.; Moore, J. S.; White, S. R. *Nat. Mater.* **2007**, *6*, 723−733.
(9) Toohey, K. S.; Hansen, C. J.; Lewis, J. A.; White, S. R.; Sottos, N. R. *Adv. Funct. Mater.* **2009**, *19* (9), 1399−1405.
(10) Hansen, C. J.; Wu, W.; Toohey, K. S.; Sottos, N. R.; White, S. R.; Lewis, J. A. *Adv. Mater.* **2009**, *21* (41), 4143−4147.
(11) Kolmakov, G. V.; Revanur, R.; Tangirala, R.; Emrick, T.; Russell, T. P.; Crosby, A. J.; Balazs, A. C. *ACS Nano* **2010**, *4* (2), 1115−1123.
(12) Kratz, K.; Narasimhan, A.; Tangirala, R.; Moon, S.; Revanur, R.; Kundu, S.; Kim, H. S.; Crosby, A. J.; Russell, T. P.; Emrick, T.; Kolmakov, G.; Balazs, A. C. *Nat. Nanotechnol.* **2012**, *7*, 87−90.
(13) Mason, T. G.; Weitz, D. A. *Phys. Rev. Lett.* **1995**, *74* (7), 1250−1253.

(14) Squires, T. M.; Mason, T. G. *Annu. Rev. Fluid Mech.* **2010**, *42*, 413−438.
(15) Crocker, J. C.; Valentine, M. T.; Weeks, E. R.; Gisler, T.; Kaplan, P. D.; Yodh, A. G.; Weitz, D. A. *Phys. Rev. Lett.* **2000**, *85* (4), 888−891.
(16) Dasgupta, B.; Tee, S.; Crocker, J. C.; Frisken, B. J.; Weitz, D. A. *Phys. Rev. E* **2002**, *65* (5), 051505.
(17) Lu, Q.; Solomon, M. J. *Phys. Rev. E* **2002**, *66* (6), 061504.
(18) Chen, D. T. N.; Weeks, E. R.; Crocker, J.; Islam, M. F.; Verma, R.; Gruber, J.; Levine, A.; Lubensky, T.; Yodh, A. G. *Phys. Rev. Lett.* **2003**, *90* (10), 108301.
(19) Gardel, M. L.; Valentine, M. T.; Crocker, J. C.; Bausch, A. R.; Weitz, D. A. *Phys. Rev. Lett.* **2003**, *91* (15), 158302.
(20) Dasgupta, B.; Weitz, D. A. *Phys. Rev. E* **2005**, *71* (2), 021504.
(21) Liu, J.; Gardel, M. L.; Kroy, K.; Frey, E.; Hoffman, B.; Crocker, J. C.; Bausch, A.; Weitz, D. A. *Phys. Rev. Lett.* **2006**, *96* (11), 118104.
(22) Oppong, F.; Rubatat, L.; Frisken, B. J.; Bailey, A.; De Bruyn, J. *Phys. Rev. E* **2006**, *73* (4), 041405.
(23) Jan, J.-S.; Breedveld, V. *Macromolecules* **2008**, *41* (17), 6517−6522.
(24) Larsen, T. H.; Furst, E. M. *Phys. Rev. Lett.* **2008**, *100* (14), 146001.
(25) Zhu, X.; Kundukad, B.; Van Der Maarel, J. R. C. *J. Chem. Phys.* **2008**, *129* (18), 185103.
(26) Dunstan, D. E.; Stokes, J. *Macromolecules* **2000**, *33* (1), 193−198.
(27) Mackay, M. E.; Dao, T. T.; Tuteja, A.; Ho, D. L.; Van Horn, B.; Kim, H.; Hawker, C. J. *Nat. Mater.* **2003**, *2* (11), 762−766.
(28) Tuteja, A.; Mackay, M. E.; Narayanan, S.; Asokan, S.; Wong, M. S. *Nano Lett.* **2007**, *7* (5), 1276−1281.
(29) Omari, R. A.; Aneese, A. M.; Grabowski, C. A.; Mukhopadhyay, A. *J. Phys. Chem. B* **2009**, *113* (25), 8449−8452.
(30) Egorov, S. A. *J. Chem. Phys.* **2011**, *134* (8), 084903.
(31) Guo, H.; Bourret, G.; Lennox, R. B.; Sutton, M.; Harden, J. L.; Leheny, R. L. *Phys. Rev. Lett.* **2012**, *109* (5), 055901.
(32) Kohli, I.; Alam, S.; Patel, B.; Mukhopadhyay, A. *Appl. Phys. Lett.* **2013**, *102*, 203705.
(33) Kohli, I.; Mukhopadhyay, A. *Macromolecules* **2012**, *45*, 6143−6149.
(34) Brochard Wyart, F.; De Gennes, P. G. *Eur. Phys. J. E* **2000**, *1* (1), 93−97.
(35) Cai, L.-H.; Panyukov, S.; Rubinstein, M. *Macromolecules* **2011**, *44* (19), 7853−7863.
(36) Yamamoto, U.; Schweizer, K. S. *J. Chem. Phys.* **2011**, *135* (22), 224902.
(37) Kalathi, J. T.; Yamamoto, U.; Schweizer, K. S.; Grest, G. S.; Kumar, S. K. *Phys. Rev. Lett.* **2014**, *112* (10), 108301.
(38) Berry, H.; Chaté, H. *Phys. Rev. E* **2014**, *89* (2), 022708.
(39) Lu, B.; Denton, A. R. *J. Phys.: Condens. Matter* **2011**, *23* (28), 285102.
(40) Dix, J. A.; Verkman, A. S. *Annu. Rev. Biophys.* **2008**, *37*, 247−263.
(41) Wong, I. Y.; Gardel, M. L.; Reichman, D. R.; Weeks, E. R.; Valentine, M. T.; Bausch, A. R.; Weitz, D. A. *Phys. Rev. Lett.* **2004**, *92* (17), 178101.
(42) Banks, D. S.; Fradin, C. *Biophys. J.* **2005**, *89* (5), 2960−2971.
(43) Szymanski, J.; Weiss, M. *Phys. Rev. Lett.* **2009**, *103* (3), 038102.
(44) Yu, Y.; Anthony, S. M.; Bae, S. C.; Granick, S. *J. Phys. Chem. B* **2011**, *115* (12), 2748−2753.
(45) Zustiak, S. P.; Nossal, R.; Sackett, D. L. *Biophys. J.* **2011**, *101* (1), 255−264.
(46) Sokolov, I. M. *Soft Matter* **2012**, *8* (35), 9043−9052.
(47) Thiel, F.; Flegel, F.; Sokolov, I. M. *Phys. Rev. Lett.* **2013**, *111* (1), 010601.
(48) Flory, P. J.; Fox, T. G. *J. Am. Chem. Soc.* **1951**, *73*, 1904−1908.
(49) Dobrynin, A. V.; Colby, R. H.; Rubinstein, M. *Macromolecules* **1995**, *28* (6), 1859−1871.
(50) Crocker, J. C.; Grier, D. G. *J. Colloid Interface Sci.* **1996**, *179* (1), 298−310.
(51) Boris, D. C.; Colby, R. H. *Macromolecules* **1998**, *31* (17), 5746−5755.
(52) Phillies, G. D. J. *Macromolecules* **1986**, *19* (9), 2367−2376.
(53) Sprakel, J.; Van Der Gucht, J.; Cohen Stuart, M. A.; Besseling, N. A. M. *Phys. Rev. Lett.* **2007**, *99* (20), 208301.
(54) Sprakel, J.; Van Der Gucht, J.; Cohen Stuart, M. A.; Besseling, N. A. M. *Phys. Rev. E* **2008**, *77* (6), 061502.
(55) Li, J.; Li, W.; Huo, H.; Luo, S.; Wu, C. *Macromolecules* **2008**, *41* (3), 901−911.